

A way to identify whether a DFT gap is from right reasons or error cancellations: The case of copper chalcogenides

Jiale Shen,¹ Haitao Liu,^{2,3} and Yuanchang Li¹

¹*Key Lab of advanced optoelectronic quantum architecture and measurement (MOE), and Advanced Research Institute of Multidisciplinary Science, Beijing Institute of Technology, Beijing 100081, China*

²*Institute of Applied Physics and Computational Mathematics, Beijing 100088, China*

³*National Key Laboratory of Computational Physics, Beijing 100088, China*

(*Electronic mail: yuancli@bit.edu.cn)

(Dated: 12 June 2024)

Gap opening remains elusive in copper chalcogenides (Cu_2X , $X = \text{S}, \text{Se}$ and Te), not least because Hubbard + U , hybrid functional and GW methods have also failed. In this work, we elucidate that their failure originates from a severe underestimation of the $4s$ - $3d$ orbital splitting of the Cu atom, which leads to a band-order inversion in the presence of an anionic crystal field. As a result, the Fermi energy is pinned due to symmetry, yielding an invariant zero gap. Utilizing the hybrid pseudopotentials to correct the underestimation on the atomic side opens up gaps of experimental magnitude in Cu_2X , suggesting their predominantly electronic nature. Our work not only clarifies the debate about the Cu_2X gap, but also provides a way to identify which of the different methods really captures the physical essence and which is the result of error cancellation.

I. INTRODUCTION

Understanding the nature of the gap and accurately calculating its size have been one of the central themes of modern electronic structure theory, especially in the study of transition-metal compounds with exotic physics and promising applications¹⁻⁴. Unfortunately, this remains a formidable challenge for today's widely used calculation methods. For example, density-functional theory (DFT) systematically underestimates gaps and can even incorrectly predict semiconductors as metals^{5,6}. To address this problem, methods such as Hubbard + U , hybrid functionals and GW have been developed based on DFT, which typically reproduce the experimental gap under certain conditions⁷⁻¹⁰. However, there is a lack of ways to identify which truly capture the physical essence and which are the result of error cancellation.

Copper chalcogenides (Cu_2X , $X = \text{S}, \text{Se}$ and Te) are a class of low-cost and environmentally friendly materials for thermoelectric and photovoltaic applications^{11,12}. Their interesting phase shares a common structure in which the X atoms form an ordered lattice skeleton while the Cu atoms are randomly distributed on tetrahedral interstitial sites formed by the X atoms. It has been known for a long time that Cu_2X has an optical gap in the range $1.08\sim 1.23$ eV¹³⁻¹⁵, yet theoretical study of its electronic structure has been hindered by the complexity of its crystal structure. Until 2007, Lukashev et al. propose a highly symmetric antiferroite model that has since been widely adopted¹⁶⁻¹⁸. Using this perfect crystal structure, their LDA calculation yields a zero gap characterized by the intersection of the conduction and valence bands at the Γ point. This is not surprising, since it had become generally known by then that DFT underestimates the gap, especially given the presence of the transition-metal Cu. What is really surprising is that the Hubbard + U , hybrid functionals and quasiparticle self-consistent GW calculations also feature the same zero gap¹⁷⁻¹⁹. Remarkably, the self-consistent GW succeeds in solving gap underestimation of analogous monovalent cop-

per halides and oxides^{20,21} that have long been notorious for DFT and its derivatives. In view of the failure of GW , Lukashev et al. explore the possibility of opening the gap through a "so-called structural mechanism" by considering the deviation of the realistic structure from the antiferroite model¹⁷. However, their calculations show that this would only yield about half of the experimental gap. Since then, there has been much debate as to whether the gap of Cu_2X is opened by an electronic or structural mechanism. In 2012, Xu et al.²² use the HSE to compute much more realistic structures, obtaining gaps that are almost identical to the experiments. This seems to indicate that the structural mechanism is indeed at work. However, in 2014, Zhang et al.¹⁹ find that the mBJ + U calculations can open up $0.5\sim 1.2$ eV gap for the perfect antiferroite structure, reigniting the controversy.

Does the gap of Cu_2X arise from an electronic mechanism or from a structural mechanism due to the over-simplified antiferroite model? Is there some commonality in gap underestimation for monovalent copper chalcogenides, halides and oxides? Despite years of attention, these mysteries remain unknown.

Perhaps it is both electronic and structural mechanisms that are responsible for the gap. Under such circumstances, ones must quantitatively compare the respective sizes of the two. This requires the electronic structure calculation to give not only the right result (gap value), but also the right result for the right reason (gap physics). In practice, a straightforward way of tackling the gap controversy is to treat the "true" gap of the antiferroite structure obtained under the correct gap physics as the contribution from the electronic mechanism. The difference between this and the experimental value is then used to roughly assess the magnitude of the structural contribution. Nevertheless, DFT-based methods such as aforementioned HSE and mBJ + U both include tunable parameters. Based solely on the fact that the gap value is reproduced, it is not possible to determine whether this is a result of the tunable parameters or whether the gap physics is truly revealed.

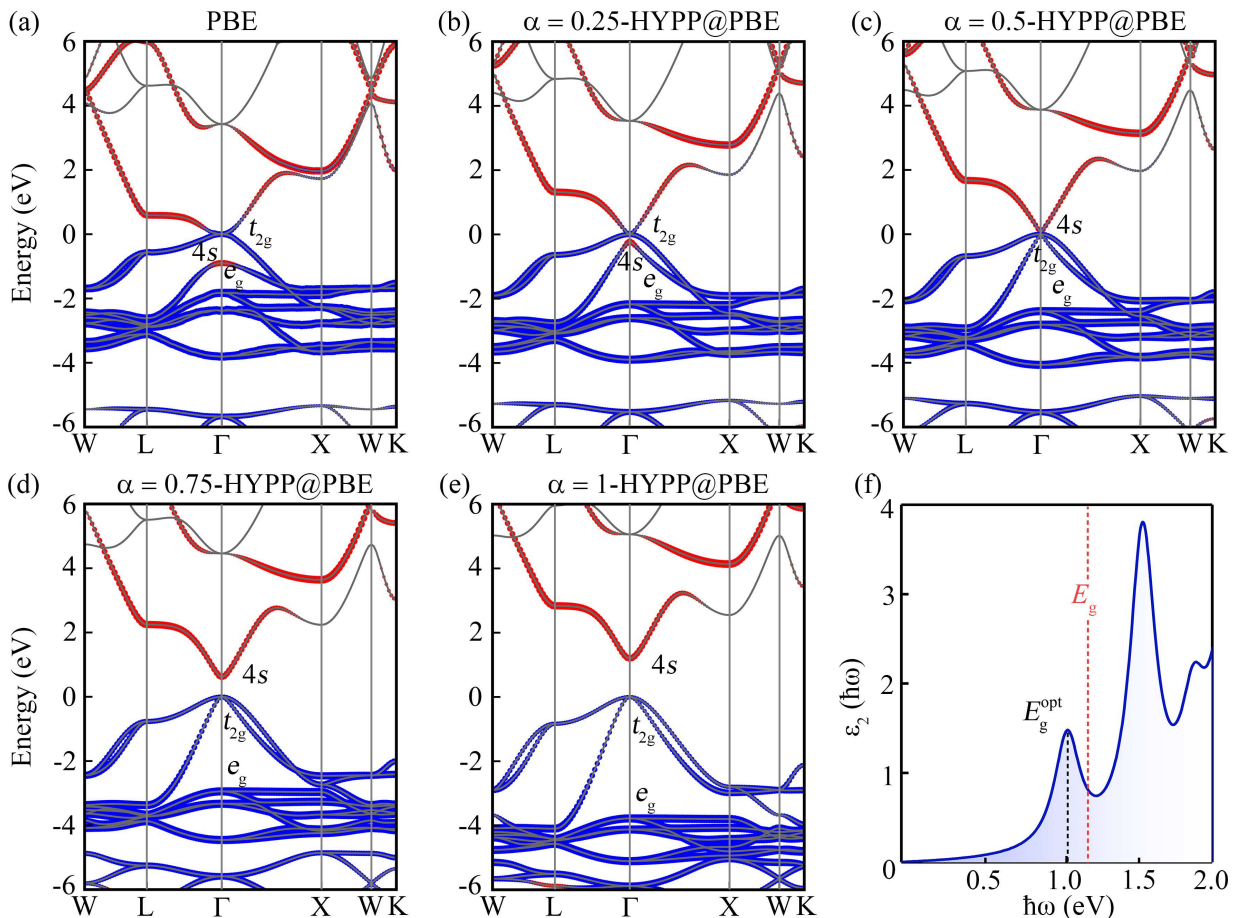


FIG. 1. Band structures of Cu_2S by (a) standard PBE, (b)-(e) HYPP@PBE at different α . Red and blue dots represent the contributions from Cu $4s$ and $3d$ orbitals, respectively. Three characteristic bands are marked as t_{2g} , $4s$ and e_g at the Γ point. The valence band maximum is set as energy zero. (f) Imaginary part of the BSE dielectric function calculated on top of $\alpha = 1$ -HYPP@PBE results. Black and red dashed lines denote optical and fundamental gaps, respectively.

Therefore, the key to resolving the Cu_2X gap controversy lies in identifying the calculation of correctly capturing the gap physics, which is what this work is addressing.

In this work, we find that the presence or absence of a computational gap in Cu_2X depends on the competition between the $4s$ - $3d$ splitting of Cu atoms and the crystal field effect of anions. A severe underestimation of the former causes $3d$ and $4s$ band-order inversion and the Fermi energy pinning by symmetry, producing a zero gap. This is the reason why many DFT-based methods fail to open a gap. Using hybrid pseudopotentials (HYPPs) corrects the atomic splitting to the experimental value, which simultaneously opens a gap of the experimental magnitude in Cu_2X . As such, it not only gets the right results, but more importantly, it gets the right results for the right reasons. In contrast, neither Hubbard + U nor hybrid functional calculations can correct for both atom-side and solid-side underestimations, implying an error cancellation. These results indicate a primarily electronic nature of the Cu_2X gap.

II. METHODOLOGY AND MODELS

Three cross PP@functional calculations were performed using the Quantum Espresso package²³, i.e., HYPPs²⁴ with PBE functional²⁵, PBE PPs with PBE + U ²⁶ and HSE functional⁹, respectively denoted as HYPP@PBE, PBE@PBE U and PBE@HSE below, for clarity. The HYPPs²⁴ were derived from the PBE0 functional, but with the amount of exact-exchange set as an adjustable parameter α . Throughout this work, they involved only the Cu element and were constructed with the OPIUM code²⁷ using the same parameters as before²⁸⁻³¹. For other elements, the norm-conserving Vanderbilt PPs³² were used with energy cutoffs of 60 Ry. A $12 \times 12 \times 12$ k -grid was used for the Brillouin zone sampling. Spin-orbit coupling has been neglected. While test calculations show that it does have an effect on the gap size, especially for Cu_2Te containing the heavy element, it does not affect the nature of the gap, which is the concern of this work. Optical absorption spectrum was obtained by solving the Bethe-Salpeter equation (BSE)³³ using the YAMBO code³⁴, with three valence and three conduction bands to build

the BSE Hamiltonian.

III. RESULTS AND DISCUSSION

Cu_2X has similar physics except for the gap size, so Cu_2S is illustrated as an example below. Figure 1(a) shows its standard PBE band structure, which features a zero gap with the lowest conduction band and the two highest valence bands intersecting at the Γ point. Fat-band analysis shows that this triple degeneracy originates from the higher-lying t_{2g} triplet from the $3d$ -orbital splitting under the S tetrahedral field, while the Cu $4s$ resides between it and the lower-lying e_g doublet. These results are consistent with previous studies^{17–19}. Despite a zero global gap, it is customary to define the t_{2g} - $4s$ difference at the Γ point as a negative gap.

Two anomalies are worth mentioning about Fig. 1(a). On the one hand, it has been experimentally demonstrated that the oxidation state of Cu in Cu_{2-x}S is invariably +1 valence regardless of stoichiometry¹¹. Based on the unique $3d^{10}4s^1$ electronic configuration of Cu, it is natural to speculate that Cu loses $4s$ electrons to form a d^{10} semiconductor when it crystallizes with S as Cu_2S . Consequently, $4s$ and $3d$ should comprise the conduction band bottom and the valence band top, respectively, instead of the zero gap and inverted $3d$ - $4s$ band-order in Fig. 1(a). On the other hand, one can clearly see that the band-order inversion occurs only very close to the Γ point. A slight deviation will return the expected $4s$ - t_{2g} order. Such discontinuity in state characteristics is physically uncommon.

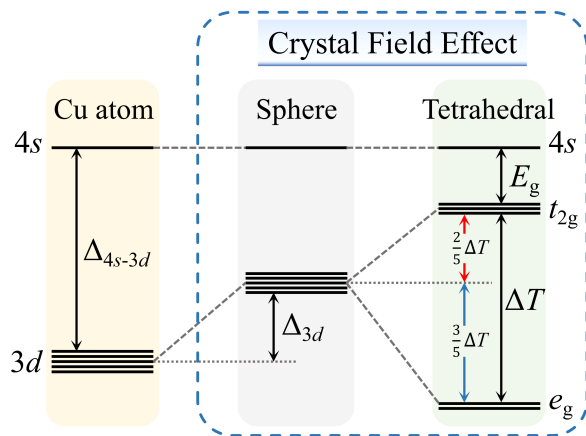


FIG. 2. Schematic of the Cu_2X gap as a result of the competition between the $4s$ and $3d$ energy splitting Δ_{4s-3d} of Cu atom and the anionic crystal field effect. Upon crystallization into Cu_2X , the crystal field formed by the four surrounding anions narrows the splitting by $\Delta_{\text{cf}} = \Delta_{3d} + \frac{2}{5}\Delta T$ in two ways. Assuming that the charge is uniformly distributed over a sphere, electrostatic repulsion causes the $3d$ orbitals to rise Δ_{3d} as a whole. Consider further that the charges are distributed tetrahedrally. The $3d$ orbitals are split into a higher-lying t_{2g} triplet and lower-lying e_g doublet with an energy difference of ΔT . If Δ_{4s-3d} surpasses the crystal field effect, E_g is positive. Otherwise, t_{2g} will lie above the $4s$, resulting in a negative E_g .

Figures 1(b)-1(e) show the band structures by different Cu HYPPs of $\alpha = 0.25, 0.50, 0.75,$ and 1 , in combination with PBE functional. One can see that Cu $4s$ rises with increasing α , from below t_{2g} at $\alpha = 0$ to coinciding with it at $\alpha = 0.5$. Continuing to increase α , a global gap appears and gradually increases. Once the gap opens, t_{2g} and $4s$ comprise the valence band top and the conduction band bottom, respectively. At $\alpha = 1$, the gap reaches 1.20 eV, agreeing almost perfectly with the experimental 1.21 eV¹³. Bader charge analysis shows that as α increases from 0 to 1 , there is a small increase about 10% in charge transfer from Cu to S.

We further calculate the optical absorption spectrum on top of the $\alpha = 1$ -HYPP@PBE band, as plotted in Fig. 1(f). Its first peak appears at 1.06 eV, which lies within the minimum direct gap. Therefore, its optical gap is set by an exciton with a binding energy of 0.14 eV.

It is clear that the band-order of t_{2g} and $4s$ determines the presence or absence of a gap in Cu_2S . A gap exists only for a positive $4s$ - t_{2g} order. A negative $4s$ - t_{2g} order, otherwise, causes the Fermi energy pinned to t_{2g} , resulting in an invariant zero gap at the Γ point. Because the band-order depends on α , an immediate question is which α is physically reasonable. It determines whether the experimental result reproduced at $\alpha = 1$ comes from the right cause or is merely a coincidence of error cancellation.

The gap E_g of Cu_2S at the Γ point can be understood in terms of crystal field theory, as illustrated in Fig. 2. An isolated Cu atom has an energy splitting Δ_{4s-3d} between $4s$ and $3d$ states. Upon crystallization into Cu_2S , the crystal field of S will narrow the splitting by Δ_{cf} in two ways^{35–37}: 1) Assuming that the charge is uniformly distributed on a sphere around the Cu, electrostatic repulsion leads to an overall increase in the $3d$ energy by Δ_{3d} ; and 2) Further consideration of the tetrahedral charge distribution, the $3d$ degeneracy is lifted to the t_{2g} triplet and e_g doublet with an energy difference of ΔT . According to crystal field theory, t_{2g} is $\frac{2}{5}\Delta T$ higher than that of the original $3d$ ³⁸. Therefore, we have

$$E_g = \Delta_{4s-3d} - \Delta_{\text{cf}} = \Delta_{4s-3d} - \left(\Delta_{3d} + \frac{2}{5}\Delta T\right). \quad (1)$$

Equation (1) actually provides a criterion for determining whether a computational method yields the true gap. If a method does capture the gap physics, it must be able to simultaneously give the correct E_g , Δ_{4s-3d} , and Δ_{cf} . While Δ_{cf} cannot be obtained directly from experiment, both Δ_{4s-3d} and E_g can. If both are correct, it follows immediately from Equation (1) that Δ_{cf} must also be correct. Otherwise, if only E_g matches the experiment but Δ_{4s-3d} does not, this seemingly correct E_g does not represent the true gap, and is merely a coincidence of error cancellation between Δ_{4s-3d} and Δ_{cf} .

This criterion makes physical sense. The Hohenberg-Kohn theorem states that the ground-state electron density of an interacting electron system is uniquely characterized by the external potential⁴⁰. Changing the PP means changing the external potential felt by the Cu valence electrons. Here the Δ_{4s-3d} serves in a way as a test of the correctness of the external potential. If a method gets the correct Δ_{4s-3d} and E_g on both the atom side and the solid side, there is no doubt that the cor-

rect gap is obtained under the correct external potential. So it is true. Otherwise, only E_g being correct and Δ_{4s-3d} being incorrect implies that the gap is obtained under an incorrect external potential. Thus, it is an error-canceling coincidence and the true gap obtained under the correct external potential will no longer be E_g .

The calculated Δ_{4s-3d} , Δ_{3d} , ΔT and E_g with different HYPPs are listed in Table I and compared with the experimental Δ_{4s-3d} and E_g . It can be seen that Δ_{4s-3d} by standard PBE is only 0.63 eV, which is nearly an order of magnitude smaller than the experimental 5.04 eV³⁹. It corresponds to the most negative E_g -0.91 eV. Both Δ_{4s-3d} and E_g increase monotonically with α . Interestingly, when $\alpha = 1$, $\Delta_{4s-3d} = 4.72$ and $E_g = 1.20$ eV reproduce the experimental values (5.04 and 1.21 eV) almost simultaneously. Since Δ_{4s-3d} is still slightly underestimated, it makes sense and physical logic that E_g is also slightly underestimated. Now we know that the conventional DFT underestimation of the Cu_2S E_g is due to an underestimation of Cu Δ_{4s-3d} , which incorrectly results in it being smaller than the $3d$ energy rise induced by the S crystal field. This consequently reverses the band-order of t_{2g} and $4s$, producing a negative E_g and pinning the Fermi energy to the t_{2g} by symmetry. In light of the criterion established above, the ability of using HYPPs to synchronously correct the underestimations of Δ_{4s-3d} on the atom side and E_g on the solid side indicates that the $\alpha = 1$ -HYPP@PBE indeed captures the gap physics. Therefore, the produced $E_g = 1.20$ eV is the right result for the right reason, representing the true gap of the antiferroite structure.

We also performed PBE@PBEU and PBE@HSE calculations and the results are summarized in Table I for comparison. Both Δ_{4s-3d} and E_g show a tendency to increase with increasing U or α . Specifically, for the PBE@PBEU, $\Delta_{4s-3d} = 3.77$ eV at $U = 7$ eV is underestimated by 1.27 eV, corresponding to a negative E_g of -0.14 eV. Increasing U to 10 eV, $\Delta_{4s-3d} = 5.14$ eV is already slightly higher than the experimental 5.04 eV, but opens only a tiny E_g of 0.09 eV. To open the experimental $E_g \sim 1$ eV, U would have to reach 45 eV, at which point Δ_{4s-3d} is four times larger than the experiment. The ineffectiveness of applying U can be understood as a consequence of the rapid increase in Coulomb repulsion with increasing U , which leads to a severe overestimation of the S crystal field effect, thereby canceling out the vast majority of the Δ_{4s-3d} increase. The presence of such depletion causes E_g to grow extremely slowly with increasing U .

Previous study¹⁸ has found that the PBE@HSE E_g for Cu_2Se is sensitive to the range separation parameter ω , which is non-zero only when $\omega < 0.2 \text{ \AA}^{-1}$. Here, we fix $\omega = 0.106 \text{ \AA}^{-1}$ for HSE06⁹ but change the exact exchange weight α . It can be seen from Table I that the PBE@HSE at typical $\alpha = 0.25$ gives $\Delta_{4s-3d} = 2.65$ and $E_g = 0.42$ eV, respectively, both of which are significantly underestimated. At $\alpha = 0.375$, $E_g = 1.12$ eV is close to the experimental 1.21 eV¹³, but the corresponding $\Delta_{4s-3d} = 3.70$ eV is still underestimated by 1.34 eV. At $\alpha = 0.50$, $\Delta_{4s-3d} = 4.77$ eV approaches the experimental 5.04 eV³⁹, but $E_g = 1.65$ eV already exceeds the experimental 1.21 eV by nearly 40%. Even taking excitons into account (borrowing the binding energy of 0.14 eV from above

TABLE I. The calculated Δ_{4s-3d} , Δ_{3d} , ΔT and E_g from standard PBE and different HYPPs (HYPP@PBE), PBE + U (PBE@PBEU) and HSE (PBE@HSE) calculations, along with the known experimental values for comparisons. The value of α denotes the portion of exact exchange used for HYPPs or HSE functionals. All units are in eV.

Methods	Δ_{4s-3d}	Δ_{3d}	ΔT	E_g
Experiment	5.04 ³⁹	—	—	1.21 ¹³
PBE	0.63	0.81	1.83	-0.91
$\alpha=0.25$ -HYPP@PBE	1.59	0.94	2.17	-0.22
$\alpha=0.50$ -HYPP@PBE	2.13	1.11	2.39	0.06
$\alpha=0.75$ -HYPP@PBE	3.27	1.47	2.94	0.62
$\alpha=1.00$ -HYPP@PBE	4.72	2.01	3.78	1.20
PBE@PBEU=7	3.77	2.49	3.54	-0.14
PBE@PBEU=10	5.14	3.27	4.46	0.09
PBE@PBEU=45	21.67	13.28	18.37	1.04
PBE@HSE- $\alpha=0.25$	2.65	1.24	2.47	0.42
PBE@HSE- $\alpha=0.375$	3.70	1.44	2.85	1.12
PBE@HSE- $\alpha=0.50$	4.77	1.69	3.57	1.65

$\alpha = 1$ -HYPP@PBE calculation), the relative error is still 25%. These point out that the PBE@HSE, unlike the U effect, tends to underestimate the crystal field effect of S, and thus gives the largest E_g for the same Δ_{4s-3d} .

Above results clearly show that neither PBE@PBEU nor PBE@HSE can yield the correct Δ_{4s-3d} and E_g at the same time. Within typical parameter ranges ($U < 10$ eV and $\alpha < 0.3$), both methods tend to underestimate Δ_{4s-3d} , which leads to an underestimation of E_g . The PBE@PBEU opening E_g by 0.09 eV at $U=10$ eV suggests that the Cu_2S gap is largely irrelevant to Mott physics. Even leaving aside the physical plausibility of the parameters, the gap calculated by the PBE@HSE for the antiferroite structure under the correct external potential is already significantly larger than the experimental value (see PBE@HSE- $\alpha = 0.50$ in Table I). This suggests that the PBE@HSE is not suitable for resolving the gap controversy, since at this point it implies a clearly implausible negative structural contribution. Putting these together, neither PBE@PBEU nor PBE@HSE correctly captures the gap physics of Cu_2S , so even if they happen to get the correct E_g , it is not true but only the result of an error cancellation.

In order to fully understand the gap nature, we have also investigated the following three structural effects. First, the Cu atoms deviate from high-symmetry positions in the antiferroite structure. Despite the dependence on the direction and magnitude of the deviation, our test calculations with $\alpha = 1$ -HYPP@PBE show that this induces a gap correction of no more than 0.1 eV. This finding is consistent with a previous study¹⁷. Second, we have directly calculated the monoclinic, hexagonal, and cubic Cu_2S with the realistic structures using $\alpha = 1$ -HYPP@PBE and obtained gaps of 1.56, 1.43 and 1.30 eV, respectively. They are at the same level as the HSE²² and experimental results. Given that the electronic mechanism opens a gap of 1.20 eV, the structural mechanism is indeed of secondary importance. Third, we have evaluated the effect of copper stoichiometry in terms of cubic $\text{Cu}_{1.8}\text{S}$ ^{17,22}.

The standard PBE opens a gap of 0.42 eV while our $\alpha = 1$ -HYPP@PBE opens a gap of 1.68 eV. Note that it has an experimental gap of 1.75 eV⁴¹. Compared to GW 1.06 eV¹⁷ and HSE 1.20 eV²², our result is clearly much better.

Performing $\alpha = 1$ -HYPP@PBE calculations on Cu₂Se and Cu₂Te open direct gaps at the Γ point of 0.75 and 1.39 eV, respectively, compared to their experimental values of 1.23 eV¹⁴ and 1.08 eV¹⁵. The former is underestimated by almost 40%, signifying an important complementary role of Cu structural disorder. Indeed, an extremely strong liquid-like effect is experimentally found in Cu₂Se¹². In contrast, the relatively small overestimation for Cu₂Te comes from our neglect of the spin-orbit coupling¹⁹. Hence, its gap should originate from an electronic mechanism.

IV. CONCLUSIONS

In summary, we compare the electronic structure of Cu₂X calculated with HYPPs, Hubbard + U and hybrid functionals, with a focus on the gap nature. While each can reproduce experimental gaps under specific parameters, only the $\alpha = 1$ -HYPP@PBE method complies with the right results for the right reasons. The other two suffer from significant error cancellations. Consequently, it is easy to understand that the same $\alpha = 1$ -HYPP also works well for other monovalent copper halides²⁸ and delafossite oxides²⁹. Our results indicate that the time-averaged antifluorite model reflects the gap physics of Cu₂S and Cu₂Te well due to their predominantly electronic nature. However, for Cu₂Se, deviations from the antifluorite model and liquid-like structural disorder must be taken into account.

Traditionally, the PPs are used to reproduce all-electron results with higher efficiency, so those consistent with exchange correlations are customarily employed. In practice, there is another side of the coin for PPs as well, as their specific form also substantially affects the external potential where the valence electrons are located. This, however, has not yet been emphasized. The Hohenberg-Kohn theorem restricts the DFT to producing the correct ground-state properties only at the correct external potential. If calculations are performed at the wrong external potential, DFT fails in principle. Utilizing PPs to correct the external potential from the atomic side provides a new perspective on solving the persistent gap problem that has long plagued the DFT field.

ACKNOWLEDGMENTS

This work was supported by the Ministry of Science and Technology of China (Grant Nos. 2023YFA1406400 and 2020YFA0308800) and the National Natural Science Foundation of China (Grant Nos. 12074034 and 11874089).

AUTHOR DECLARATIONS

Conflict of Interest

The authors have no conflicts to disclose.

Author Contributions

Jiale Shen: Formal analysis (equal); Investigation (equal); Software (equal); Validation (equal); Writing-original draft (equal). **Haitao Liu:** Formal analysis (equal); Funding acquisition (equal); Methodology (equal); Validation (equal). **Yuanchang Li:** Conceptualization (equal); Formal analysis (equal); Funding acquisition (equal); Methodology (equal); Project administration (equal); Resources (equal); Supervision (equal); Validation (equal); Writing-original draft (equal); Writing-review & editing (equal).

DATA AVAILABILITY

The data that support the findings of this study are available from the corresponding author upon reasonable request.

REFERENCES

- C. N. R. Rao and G. V. S. Rao, *Transition Metal Oxides: Crystal Chemistry, Phase Transition and Related Aspects* (NSRDS-NBS, Washington, USA, 1974), Vol. 49.
- M. Imada, A. Fujimori, and Y. Tokura, "Metal-insulator transitions," *Rev. Mod. Phys.* **70**, 1039 (1998).
- Y. Tokura and N. Nagaosa, "Orbital Physics in Transition-Metal Oxides," *Science* **288**, 462 (2000).
- J. Zaanen, G. A. Sawatzky, and J. W. Allen, "Band gaps and electronic structure of transition-metal compounds," *Phys. Rev. Lett.* **55**, 418 (1985).
- M. K. Y. Chan and G. Ceder, "Efficient band gap prediction for solids," *Phys. Rev. Lett.* **105**, 196403 (2010).
- W. Q. Li, C. F. J. Walther, A. Kuc, and T. Heine, "Density functional theory and beyond for band-gap screening: performance for transition-metal oxides and dichalcogenides," *J. Chem. Theory Comput.* **9**, 2950 (2013).
- F. Tran and P. Blaha, "Accurate band gaps of semiconductors and insulators with a semilocal exchange-correlation potential," *Phys. Rev. Lett.* **102**, 226401 (2009).
- V. I. Anisimov, F. Aryasetiawan, and A. I. Lichtenstein, "First-principles calculations of the electronic structure and spectra of strongly correlated systems: The LDA + U method," *J. Phys.: Condens. Matter* **9**, 767 (1997).
- J. Heyd, G. E. Scuseria, and M. Ernzerhof, "Hybrid functionals based on a screened coulomb potential," *J. Chem. Phys.* **118**, 8207 (2003).
- M. S. Hybertsen and S. G. Louie, "Electron correlation in semiconductors and insulators: Band gaps and quasiparticle energies," *Phys. Rev. B* **34**, 5390 (1986).
- C. Coughlan, M. Ibáñez, O. Dobrozhan, A. Singh, A. Cabot, and K. M. Ryan, "Compound copper chalcogenide nanocrystals," *Chem. Rev.* **117**, 5865 (2017).
- H. Liu, X. Shi, F. Xu, L. Zhang, W. Zhang, L. Chen, Q. Li, C. Uher, T. Day, and G. J. Snyder, "Copper ion liquid-like thermoelectrics," *Nat. Mater.* **11**, 422 (2012).
- R. Marshall and S. S. Mitra, "Optical properties of cuprous sulfide," *J. Appl. Phys.* **36**, 3882 (1965).
- G. P. Sorokin, Y. M. Papshev, and P. T. Oush, "Photoconductivity of Cu₂S, Cu₂Se, and Cu₂Te," *Sov. Phys. Solid State* **7**, 1810 (1966).

- ¹⁵O. M. Hussain, B. S. Naidu, and P. J. Reddy, "Photovoltaic properties of n-CdS/p-Cu₂Te thin film heterojunctions," *Thin Solid Films* **193-194**, 777 (1990).
- ¹⁶X. Wu, C. Ming, W. Gao, J. Shi, K. Zhao, H. Wang, and Y. Y. Sun, "Effect of liquidlike cations on electronic and defect properties of solid solutions of Cu₂Te and Ag₂Te," *Phys. Rev. B*, **105**, 195206 (2022).
- ¹⁷P. Lukashev, W. R. L. Lambrecht, T. Kotani, and M. van Schilfgaarde, "Electronic and crystal structure of Cu_{2-x}S: Full-potential electronic structure calculations," *Phys. Rev. B* **76**, 195202 (2007).
- ¹⁸M. Råsaender, L. Bergqvist, and A. Delin, "Density functional theory study of the electronic structure of fluorite Cu₂Se," *J. Phys.: Condens. Matter* **25**, 125503 (2013).
- ¹⁹Y. Zhang, Y. Wang, L. Xi, R. Qiu, X. Shi, P. Zhang, and W. Zhang, "Electronic structure of antifluorite Cu₂X (X = S, Se, Te) within the modified Becke-Johnson potential plus an on-site Coulomb U," *J. Chem. Phys.* **140**, 074702 (2014).
- ²⁰M. van Schilfgaarde, T. Kotani, and S. Faleev, "Quasiparticle self-consistent *GW* theory," *Phys. Rev. Lett.* **96**, 226402 (2006)
- ²¹F. Bruneval, N. Vast, L. Reining, M. Izquierdo, F. Sirotti, and N. Barrett, "Exchange and correlation effects in electronic excitations of Cu₂O," *Phys. Rev. Lett.* **97**, 267601 (2006).
- ²²Q. Xu, B. Huang, Y. F. Zhao, Y. F. Yan, R. Noufi, and S.-H. Wei, "Crystal and electronic structures of Cu_xS solar cell absorbers," *Appl. Phys. Lett.* **100**, 061906 (2012).
- ²³P. Giannozzi, S. Baroni, N. Bonini, M. Calandra, R. Car, C. Cavazzoni, D. Ceresoli, G. L. Chiarotti, M. Cococcioni, I. Dabo, A. D. Corso, S. de Gironcoli, S. Fabris, G. Fratesi, R. Gebauer, U. Gerstmann, C. Gougoussis, A. Kokalj, M. Lazzeri, L. Martin-Samos et al. "QUANTUM ESPRESSO: a modular and open-source software project for quantum simulations of materials," *J. Phys.: Condens. Matter* **21**, 395502 (2009).
- ²⁴J. Yang, L. Z. Tan, and A. M. Rappe, "Hybrid functional pseudopotentials," *Phys. Rev. B* **97**, 085130 (2018).
- ²⁵J. P. Perdew, K. Burke, and M. Ernzerhof, "Generalized gradient approximation made simple," *Phys. Rev. Lett.* **77**, 3865 (1996).
- ²⁶S. L. Dudarev, G. A. Botton, S. Y. Savrasov, C. J. Humphreys, and A. P. Sutton, "Electron-energy-loss spectra and the structural stability of nickel oxide: an LSDA+*U* study," *Phys. Rev. B* **57**, 1505 (1998).
- ²⁷See <http://opium.sourceforge.net> for the pseudopotential generation project.
- ²⁸Y. J. Wu, Z. Y. Jiang, H. X. Tan, Y. C. Li, and W. H. Duan, "Accuracy trade-off between one-electron and excitonic spectra of cuprous halides in first-principles calculations," *J. Chem. Phys.* **154**, 134704 (2021).
- ²⁹J. L. Shen, H. T. Liu, and Y. C. Li, "On the bandgap underestimation of delafossite transparent conductive oxides CuMO₂ (M = Al, Ga and In): Role of pseudopotentials," *J. Chem. Phys.* **159**, 014706 (2023).
- ³⁰X. T. Bu and Y. C. Li, "Optical signature for distinguishing between Mott-Hubbard, intermediate, and charge-transfer insulators," *Phys. Rev. B* **106**, L241101 (2022).
- ³¹H. Tan, H. Liu, Y. Li, W. Duan, and S. Zhang, "Understanding the origin of bandgap problem in transition and post-transition metal oxides," *J. Chem. Phys.* **151**, 124703 (2019).
- ³²D. R. Hamann, "Optimized norm-conserving Vanderbilt pseudopotentials," *Phys. Rev. B* **88**, 085117 (2013).
- ³³M. Rohlfling and S. G. Louie, "Electron-hole excitations and optical spectra from first principles," *Phys. Rev. B* **62**, 4927 (2000).
- ³⁴A. Marini, C. Hogan, M. Grüning, and D. Varsano, "Yambo: an ab initio tool for excited state calculations," *Comput. Phys. Commun.* **180**, 1391 (2009).
- ³⁵H. Bethe, "Termaufspaltung in Kristallen," *Ann. Phys.* **3**, 133 (1929).
- ³⁶J. H. Van Vleck, "The group relation between the Mulliken and Slater-Pauling theories of valence," *J. Chem. Phys.* **3**, 803 (1935).
- ³⁷J. H. Van Vleck, "Valence strength and the magnetism of complex salts," *J. Chem. Phys.* **3**, 807 (1935).
- ³⁸T. Wolfram and Ş. Ellialtıođlu, *Applications of Group Theory to Atoms, Molecules, and Solids*, (Cambridge University Press, 2014), Chap. 4.
- ³⁹J. B. Mann, T. L. Meek, and L. C. Allen, "Configuration Energies of the *d*-Block Elements," *J. Am. Chem. Soc.* **122**, 5132 (2000).
- ⁴⁰P. Hohenberg and W. Kohn, "Inhomogeneous electron gas," *Phys. Rev. B* **136**, 864 (1964).
- ⁴¹L. Reijnen, B. Meester, and J. Schoonman, "Nanoporous TiO₂/Cu_{1.8}S heterojunctions for solar energy conversion," *Mater. Sci. Eng., C* **19**, 311 (2002).